Inuence on the Structure and the Molecular Mobility of Cellulose Diamine Complexes Studied by a Multiscale Experimental Approach

Agustín Rios de Anda, Axel Ettori, Yoshiharu Nishiyama, Karim Mazeau, Caroll Vergelati, Laurent Heux

Cellulose manuscript No.
(will be inserted by the editor)

Influence on the Structure and the Molecular Mobility of Cellulose – Diamine Complexes Studied by a Multiscale Experimental Approach

Agustín Rios de Anda · Axel Ettori · Yoshiharu Nishiyama · Karim Mazeau · Caroll Vergelati · Laurent Heux

Received: date / Accepted: date

Abstract In this paper the influence of diamines on the intrinsic structure and molecular mobility of cellulosic complexes is discussed. Cellulose was pre-swollen by ethylenediamine then put in contact with a series of aliphatic diamines at a stoechiometric ratio (1 *eq.* $-NH_2$ per *eq.* $-OH$). These materials were then characterized by Wide Angle X-Ray diffraction (WAXS) and solid-state ^{13}C NMR. It was observed by WAXS that diamines are able to swell cellulose along the (010) crystallographic plane and are able to modify unit cell angle γ of cellulose monoclinic structure. Moreover according to their periodicity, ordered- or disordered-phases structures were identified in such cellulosic complexes by *CP-MAS* ^{13}C NMR. *2D WISE* and T_1 relaxation time ^{13}C NMR experiments showed that complexes do exhibit molecular motions between 23 and 90°C. Modulated DSC further showed the presence of two glass transition temperatures T_g, which were attributed, in combination with the ^{13}C NMR observations through a multiscale approach, to relaxation motions internal to the diamines chemical structure and to the motion of cellulose-diamine planes respectively.

Keywords cellulose · cellulosic complexes · molecular relaxations · solid-state NMR · X-ray diffraction

A. Rios de Anda
CERMAV - Centre de Recherche sur les Macromolécules Végétales - UPR 5301, BP53 - 38041 Grenoble Cedex 9, France
Present address: Université Paris Est Créteil, CNRS, ICMPE, UMR 7182, 2 rue Henri Dunant, 94320 Thiais, France
Tel.: + 33 1 49 78 12 28
E-mail: agustin.rios-de-anda@u-pec.fr

A. Ettori, Y. Nishiyama, K. Mazeau, L. Heux
CERMAV - Centre de Recherche sur les Macromolécules Végétales - UPR 5301, BP53 - 38041 Grenoble Cedex 9, France
E-mail: laurent.heux@cermav.cnrs.fr

C. Vergelatti
Solvay in Axel'One, 85 rue des frères Perret, 69192 Saint Fons Cedex, France

1 Introduction

Cellulose, a polysaccharide, is the most abundant natural macromolecule. The interest and the research conducted on this polymer has spanned for over almost a century. As a naturally-sourced biodegradable material exhibiting outstanding mechanical properties it has found applicative uses such as in structural, biomedical, technical and packaging applications [1, 2, 3]. On the other hand, because of the strong inter- and intra-chain hydrogen bonds present in its structure [4, 5, 6], cellulose cannot be dissolved by standard solvents nor be processed by thermal methods as its glass transition temperature is higher than its decomposition temperature [7], resulting in high-pressure and solvent-induced processing methods [8, 9, 10]. This remains a major issue, since cellulose cannot be processed as a "standard" thermoplastic polymer. As such, physical and chemical modifications have been carried in cellulose to render this macromolecule processable, yielding bulk cellulose-derivate materials. As of now however, processing of native or pure cellulose remains still an open subject for research.

A proposed means to possibly overcome this is by physically swelling cellulose by integrating molecules within its structure. In order to do so, the targeted molecules should be able to strongly interact with cellulose and be able to disturb the H-bond network of this material. Indeed the strength of an amine-alcohol H bond is of *ca.* 30 kJ/mol whereas that of an alcohol-alcohol bond is of *ca.* 20 kJ/mol [11, 12, 13, 14]. Primary amines are then a good candidate as target molecules since they can interact through their $-NH_2$ functions with the $-OH$ moieties of cellulose and thus disrupt the H-bond network to some extent. Several studies on amine-cellulose complexes have been conducted with ethylenediamine (*EDA*) as a target molecule aimed to swell cellulose [15, 16, 17, 18, 19, 20, 21]. These studies have shown that *EDA* is effectively able to disrupt the H-bond network of cellulose and it is able to modify its crystalline arrangement, *i.e.* cellulose I becomes cellulose III after complexation and elimination of *EDA*. Moreover, studies on cellulosic complexes with several types of amines (such as mono-, di-, and trifunctional as well as primary, secondary or tertiary amines, hydrazine, and ammonia have been carried out in the literature [22, 23, 24, 25, 26, 27, 28, 29, 30]. Such investigations so far have dealt with the feasibility of obtaining such complexes as well as studying the influence of these amines on the crystalline structure of cellulose, specifically on the crystallographic planes, as well as the evolution of such structures with temperature. It has been observed that such molecules are capable of modyfing the inner structure of cellulose, provoking a disruption of its crystallographic planes.

In this work we seek to deepen the study of the influence of primary diamines on the intrinsic structure and the molecular mobility of cellulosic complexes that has been developed in the literature. To do so we chose a series of diamine aliphatic molecules having an increasing size ranging from 2 to 12 carbons, so as to have a well-defined periodicity. Moreover, we considered such molecules as they can form two H bonds per molecule at their extremities, thus

giving the possibility of creating "physical" bridges between cellulose chains in the complex. Moreover, having the same nature as EDA, we would expect these molecules to strongly bond to cellulose and induce a similar effect on its structure. We firstly characterized the structure of the obtained complexes by X-ray diffraction [31, 32, 33, 34, 35, 36, 37] and solid-state ^{13}C *CP-MAS* NMR [15, 16, 38, 39, 40, 41, 42, 43, 44, 45, 46, 47, 48], two techniques that have been used extensively to study cellulose. Afterwards we investigated the molecular mobility within these materials at several temperatures by *2D WISE* and T_1 relaxation time solid-state ^{13}C NMR measurements. These two techniques have been proven very efficient in characterizing the molecular dynamics of synthetic polymers [49] and we have adapted the experimental conditions in this study to examine our cellulose-diamine complexes.

2 Experiemental

2.1 Materials and cellulose-diamine complexes processing

We considered Flax cellulose as the source material for our measurements. Flax cellulose is partially crystalline (30%) and provides with a regular structure that is capable of being characterized by X-Ray diffraction. To obtain the studied cellulose-diamine complex materials, this cellulose was physically complexed with a series of diamine molecules. The molecular structure of such diamines is shown in Figure 1. These diamines are called herein *NMDA*, except for ethylene diamine (*EDA*), where *N* stands for the number of carbons between NH2 groups in the molecule and *MDA* stands for methylenediamine. All diamines were purchased from Sigma Aldrich with a purity $<$99%. Figure 1 also shows the chemical structure of cellulose with highlighted carbons of interest for the structural characterization.

The physicochemical properties of these diamines such as their melting temperature T_m, molar mass M,and distance between $-NH_2$ groups ($d_{H_2N-R-NH_2}$) within each diamine molecule are listed in Table 1. $d_{H_2N-R-NH_2}$ was obtained by modeling each molecule with the ACD/Labs ChemSketch Version 2015.2.5 freeware. Molecules were traced in this software and then a modeling and equilibrating of the molecule in 3D was undertaken before determining the distance between NH_2 groups for each molecule. This quantity $d_{H_2N-R-NH_2}$ was considered to define the molecular size of a given diamine.

To obtain the studied complexes, cellulose was firstly dried under vacuum for 1 hour at 60°C then it was pre-swollen by putting it in contact with ethylene diamine (*EDA*) for one hour at room temperature. The excess of *EDA* was eliminated by evaporating this molecule under vacuum overnight at room temperature. Afterwards the cellulose-*EDA* complex was put in contact with a given diamine introduced at molar stoechiometric proportions, *i.e.* 1 $-NH_2$ group within the diamine per $-OH$ group in cellulose. The whole was put in a round-bottom flask and heated at a temperature 20°C higher than the melting temperature of the given diamine. An inert atmosphere was needed to avoid

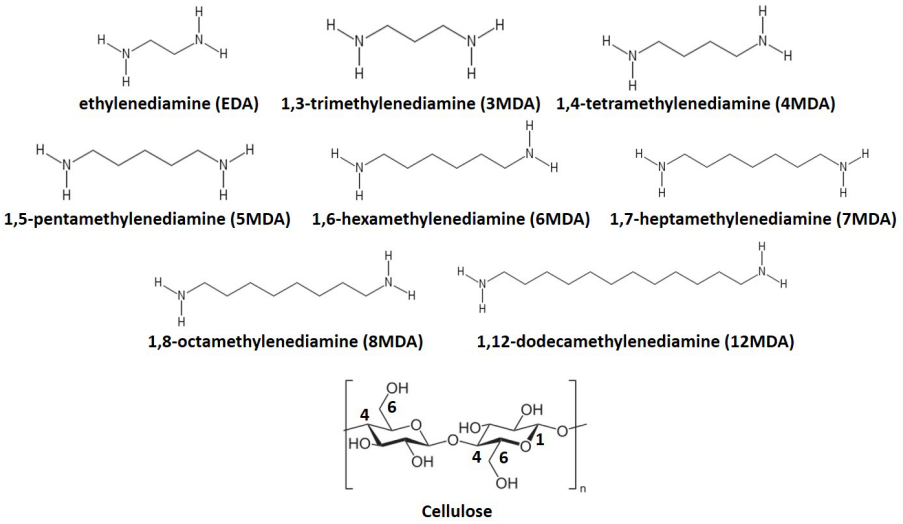

Fig. 1 Chemical structure and adopted nomenclature for the studied diamine molecules and cellulose.

Table 1 Physicochemical properties of the studied diamine molecules [50].

Diamine	T_m (°C)	M (g/mol)	$d_{H_2N-R-NH_2}$ (nm)
EDA	8	60.1	0.377
3MDA	-12	74.1	0.493
4MDA	27.5	88.2	0.620
5MDA	11.8	102.2	0.749
6MDA	39 - 42	116.2	0.868
7MDA	26 - 30	130.2	0.988
8MDA	50 - 52	144.3	1.117
12MDA	67 - 69	200.4	1.620

carbonation of the amine and was obtained by allowing a flux of dry N_2 into the flask. The complexation time was fixed at 24h, by which time the given diamine had displaced the bonded *EDA* and complexed with the cellulose.

2.2 X-Ray Diffraction characterization

To characterize the complexes inner structure, Wide Angle X-Ray diffraction measurements were carried out at our laboratory with a Philips PW3830 X-Ray Generator. The sample was placed 22cm from the X-Ray source and the detection film was placed 15cm from the sample. X-Ray beams had a KCuα filter of 1.54Å and their energy was set at 30 kV and 20 mA. Acquisition time was set at one hour per sample. The diffraction patterns were recorded on photographic films, which were later scanned and analyzed with ImageJ.

2.3 ^{13}C Solid State NMR Characterization

In order to characterize the complexes' relaxation dynamics at a molecular level, we conducted different characterization techniques using solid-state NMR ^{13}C measurements. All of these experiments were conducted in a Bruker Avance III 400 NMR equipped with a 4mm MAS DVT probe and a MAS II module. The resonance frequency for 1^H was of 400.130 MHz and that for ^{13}C was of 100.613 MHz. Samples were introduced into 4mm ZrO_2 with *KelF* caps. For all samples the ^1H excitation time was set at 5s, the $\pi/2$ pulse time was of 3.5μs and the ^1H-^{13}C cross-polarization contact time was of 1ms. In the case of samples tested at temperatures higher than room temperature, the probe was stabilized at the set temperature for an hour with the rotor spinning.

2.3.1 Cross Polarization - Magic Angle Spinning Experiments

CP-MAS (Cross Polarization - Magic Angle Spinning) measurements were conducted at room temperature and at high temperatures between 70 and 100°C. Such experiments were done so as to observe an eventual chemical shifting on the cellulose and the diamine carbons due to an increase of molecular mobility as a function of the temperature. Such experiments were done with a rotating speed of 12kHz.

2.3.2 2D WISE Experiments

2D WISE experiments, which allowed to identify and quantify the rigid and mobile fractions in cellulose-diamine complexes, were undertaken. The principle of the measurement is the following: the cross polarization from ^1H to ^{13}C is delayed compared to a standard CP-MAS experiment. This delay has as a consequence that the protons located in rigid parts will relax very quickly and thus will not be able to induce a cross polarization to the adjacent carbons. However the mobile protons will slowly relax and be able to transfer their magnetization to adjacent carbons. This will create a difference of transfer between rigid and mobile regions in the sample, which will yield different relaxation patterns. In the case of rigid zones, the pattern will be a large peak, whereas the signature of a mobile fraction will be a sharp peak [49]. Measurements were conducted on Celullose-*6MDA* and Cellulose-*7MDA* complexes at 23, 75, and 90°C with a rotating speed of 6kHz and a cross-polarization delay contact time of 1s. As an example, Figure 2 shows the *2D WISE* results for the Cellulose-6MDA complex characterized at 23°C.

2.3.3 T_1 Relaxation Experiments

Finally T_1 traverse relaxation times experiments were carried out to complement the study on the molecular mobility of the cellulose diamine complexes. For these experiments a cross-polarization between ^1H and ^{13}C is followed by a $\pi/2$ pulse and then by a delay time before the acquisition is made [49].

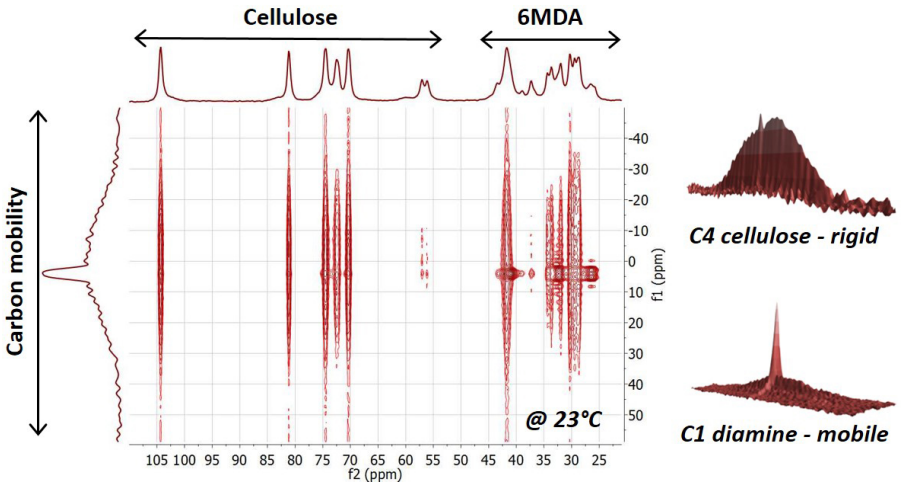

Fig. 2 *2D WISE* results for the Cellulose-6MDA complex studied at 23°C where the horizontal projection corresponds to the ^{13}C spectrum and the vertical projection corresponds to the sum of the rigid and mobile fractions of the whole complex.

Measurements were conducted on Celullose-*6MDA* and Cellulose-*7MDA* complexes at 23, 75, and 90°C with a rotating speed of 12kHz and delay times of 0.00001, 0.2, 0.4, 0.8, 1.6, 3.2, 6.4, and 12.8 seconds.

2.4 Modulated DSC Characterization

DSC measurements were conducted on a TA Q2000 in the temperature - modulated mode. Cellulose-diamine complex samples were put in non-hermetic aluminum pans and heated at 3°C/min with a temperature modulation of 2°C every 60s from 25 to 150°C. This method has proven to allow the observation of glass transition phenomena in polymers for which it is difficult to measure this temperature [51, 52, 53, 54]. Three measurements per complex were done with the T_g for each sample being taken at the inflection point of the heat capacity step in the Reversing Heat Flow signal.

3 Results and Discussion

3.1 Structural characterization by X-Ray diffraction

The inner structure of cellulose-diamine complexes was studied by X-Ray diffraction at room temperature. From the diffraction patterns, cell parameter values corresponding to the $d(010)$ plane of cellulose was extracted. It is known in the litterature that this is the plan affected by the presence of diamines [15, 16, 17, 18, 19, 20, 21, 22, 23, 24, 25, 26, 27, 28, 29, 30]. The numerical value of the cell parameter for the $d(010)$ plane was then plotted

in Figure 3a as a function of the distance between $-NH_2$ groups in a diamine molecule $d_{H_2N-R-NH_2}$. Figure 3a does not include the values for EDA, as this molecule has a larger stoichiometric ratio (*i.e.* 2 molecules of EDA per $-OH$ function in cellulose) than the rest of the diamines (*i.e.* 1 $-NH_2$ of diamine per $-OH$ function in cellulose).

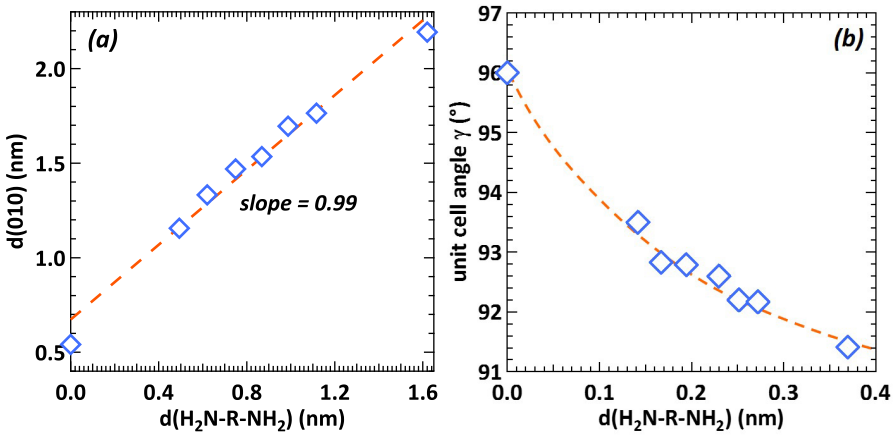

Fig. 3 (a) Distance of the $d(010)$ crystallographic plane of cellulose and (b) unit cell angle γ plotted as a function of the distance between $-NH_2$ groups in a diamine molecule $d_{H_2N-R-NH_2}$. The dashed lines are guides for the eyes.

It is shown in Figure 3a that for the cellulose-diamine complexes, the increase of the cell parameter in the $d(010)$ plane varies linearly with $d_{H_2N-R-NH_2}$. Moreover it is seen that the slope has the value of the unity, which would mean that the increase in the cell parameter of the $d(010)$ plane is directly proportional to the diamine size and the molar stoichiometry of the complexes. To further this analysis, from the diffraction patterns, the unit cell angle γ for each complex was determined from Equation 1. Indeed, as the unit cell of cellulose I crystals is monoclinic, thus γ is different from 90° [20]. The obtained values of γ are plotted in Figure 3b as a function of $d_{H_2N-R-NH_2}$ for each cellulose-amine complex.

$$\gamma = 180° - \left(\frac{d^2_{1\bar{1}0}}{d^2_{100} + d^2_{010} + 2d_{100}d_{010}} \right) \tag{1}$$

Figure 3b shows that the value of γ decreases with $d_{H_2N-R-NH_2}$, *i.e.* an increasing diamine size, and leans towards 90°. This would mean that the crystalline cell unit tends to become an orthorhombic structure when diamines are present in cellulose. It is important to note that the orthorhombic structure is more symmetric than the monoclinic cell. This confirms the results observed in the literature, showing that diamines are able to effectively modify the

intercalary planes of cellulose, prompting the modification of its crystalline structure.

3.2 Structural characterization by ^{13}C CP-MAS NMR

The obtained Cellulose-diamine complexes were then characterized by ^{13}C CP-MAS NMR at room temperature. Special interest was paid on the cellulose chemical shift region. The obtained spectra for such complexes and for neat cellulose are shown in Figure 4.

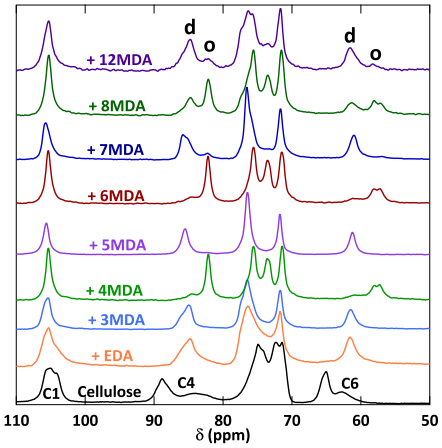

Fig. 4 ^{13}C CP-MAS NMR spectra zoomed on the cellulose chemical shifts obtained at room temperature for neat cellulose and for the studied cellulose-diamine complexes.

A focus on the chemical shifts corresponding to the *C4* and *C6* carbons in cellulose was made. The NRM spectra plotted in Figure 4 show that in presence of diamines, the peaks corresponding to the *C4* (90 ppm) and *C6* (65 ppm) carbons are deshielded, and that the chemical shifts of the remainin cellulose carbons (76-70 ppm) are also modified. This is a signature of the effective complexation of diamines on cellulose [43]. Moreover it is observed that two peaks are observed for the *C4* and *C6* carbons depending on the diamine structure. These peaks are believed to correspond to disordered and ordered phases within the cellulose complexes. The peak corresponding to the disordered phase appears at around 85 ppm whereas the ordered peak signal appears at around 82ppm. This has been already determined by Wormald *et.al.* [43] where they observed the same chemical shifts in the *C4* and *C6* cellulose carbons for samples having undergone water immersion-drying and mechanical tension cycles. In this work, a pattern is observed and is the following: for even-numbered diamines both orderered and disordered peaks are observed, with the ordered intensity being larger and when the size of the diamine increases, the ordered peak intensity decreases. On the other hand, for

odd-numbered diamines, the disordered peak intensity is the largest and that when the diamine size increases, an ordered peak appears and the intensity of the disordered signal decreases. To summarize and quantify these observations, the ordered phase ratio for each complex was calculated by integrating the organized and disorganized peak surfaces. These values are shown in Table 2.

Table 2 Ordered phase ratio calculated from ^{13}C CP-MAS NMR in Figure 4 for each cellulose-diamine complex.

Cellulose complex	Ordereed phase (%)
Neat	-
+ EDA	0
+ 3MDA	0
+ 4MDA	90
+ 5MDA	0
+ 6MDA	87
+ 7MDA	9
+ 8MDA	64
+ 12MDA	22

To explain this periodicity, the proposed hypothesis is based on what has been observed for even- and odd-numbered polymers such as polyamides [55, 56] as well as on liquid crystals and organic molecules organizing through H-bonds [57, 58, 59, 60, 61]. For instance, it is well known that even even-numbered polyamides have higher glass transition and melting temperatures as well as a larger crystalline fraction than those of odd-numbered polyamides. This is due to the fact that because of the space arrangement of polyamide chains, even-numbered polymers can form a >C=O | | | HN- hydrogen bond for every amide in the structure whereas this number is cut by half for odd-numbered polyamides. Such similar effects are observed in liquid crystals and organic molecules bearing H bonding groups. In this case, even-numbered diamines yield a preponderant ordered phase could be possible because these molecules are favored to H-bond with two cellulose chains at a time without modifying their canonical geometrical orientation. Odd-numbered diamines however will have to modify this structure and twist in space onto less favorable orientations in order to form two H bonds at once, giving a more disordered structure.

3.3 Molecular mobility by ^{13}C NMR

2D WISE ^{13}C NMR experiments were then conducted on the Cellulose-6MDA and Cellulose-*7MDA* complexes at 23, 75 and 90°C. To study the evolution of the complexes molecular mobility, the C4 and C6 carbons of cellulose (*i.e.* Figure 1) and the carbons immediately adjacent to the $-NH_2$ functions for *6MDA* and *7MDA* were chosen. Their molecular mobility was extracted from

their individual 1D rigid-mobile projection given by *2D WISE* ^{13}C NMR experiments. An example of such projections for Cellulose C4 carbon and the carbons immediately adjacent to the $-NH_2$ functions of 6MDA is given in Figure 5.

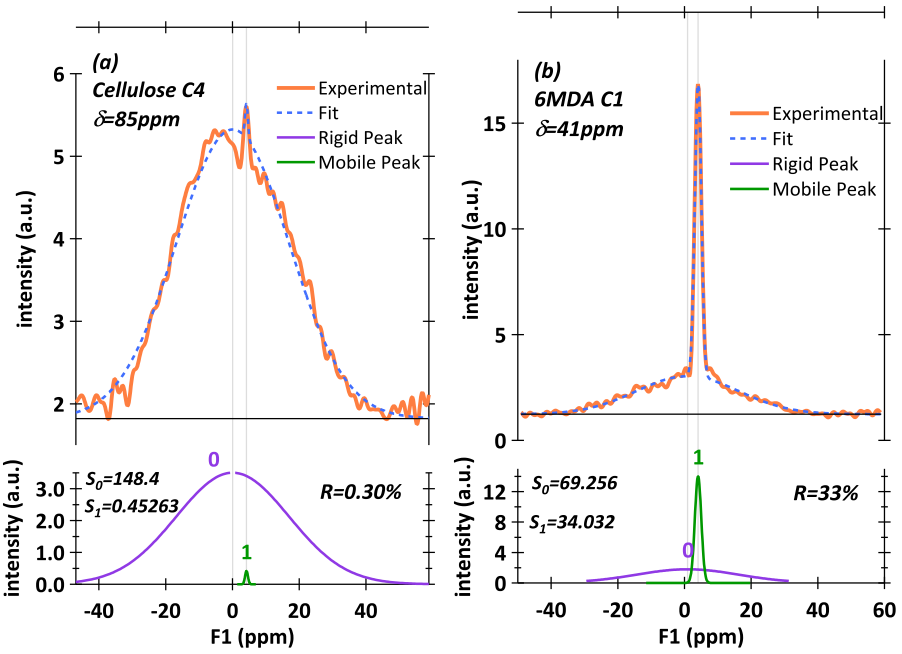

Fig. 5 ^{13}C 1D rigid-mobile projection obtained by *2D WISE* ^{13}C NMR experiments for (a) the C4 carbon of cellulose (i.e. Figure 1) and (b) the carbons immediately adjacent to the $-NH_2$ functions for *6MDA*. The projections are deconvoluted into rigid (large peak) and mobile (sharp peak) components fitted by the IgorPro Version 6.32 software.

Figure 5 further shows the undertaken data analysis. The 1D projections were deconvoluted into two Gaussian peaks fitted by the IgorPro Version 6.32 software. The proportion of rigid and mobile fractions was then calculated by dividing the surface of the mobile peak over the total surface for both the rigid and mobile peaks. These results are listed in Table 3.

Table 3 shows that the selected cellulose carbons in both complexes remain mainly rigid even at 90°C. It is important to mention that because samples are spun at 6kH, it might be possible that if there is a molecular relaxation corresponding to the movements of cellulose within the complex, it would be higher than 90°C and that this temperature would be shifted of at least 25°C towards higher temperatures, *ca.* 6°C per frequency decade according to the time-temperature equivalence principle [62]. In the case of diamines, it is seen in Table 3 that at room temperature these molecules have a non-negligible mobility fraction, which would mean that inner motions within diamines have

Table 3 Mobile fractions for selected cellulose carbons (C1, C4, C6, *i.e.* Figure 1) and for the carbons immediately adjacent to the $-NH_2$ functions in *6MDA* and *7MDA*, for these cellulose-diamine complexes calculated from *2D WISE* ^{13}C NMR experiments at 23, 75 and 90°C.

			Cellulose-6MDA			Cellulose-7MDA		
	Carbon	δ (ppm)	23°C	75°C	90°C	23°C	75°C	90°C
Cellulose	C1	104	0.3	1.0	0.6	1.0	1.1	1.8
	C4	85	0.3	0.4	0.4	0.0	0.7	0.0
	C6	57	1.0	0.9	0.6	2.1	2.6	3.0
Diamine	Adjacent to $-NH_2$	42	33.0	43.3	55.2	33.8	36.9	40.1

already relaxed, *i.e.* that their proper glass transition temperature T_g has been reached and passed over. To explain this phenomenon let us assimilate the studied cellulose-diamine complexes to high density polyethylene (HDPE). Indeed, the studied diamines could be considered as oligomeric polyethylene (i.e. $-(CH_2-CH_2)_n$) chains. HDPE has a high crystalline fraction (ca. 80%), so PE chains in the amorphous phase are highly constrained. The glass transition temperature of this phase increases from -120°C for an amorphous PE to between -20 and 0°C for HDPE, as has been observed by DMA [63]. In the case of the studied cellulose-diamine complexes, as *2D WISE* ^{13}C NMR measurements are carried out well over this range of temperature, it would be likely that a fraction of diamines has indeed relaxed. Furthermore, Table 3 shows that the mobile fraction of amine increases with temperature. This would mean that the diamines within the complex are somehow mobile at temperatures between 23 and 90°C and that a higher amount of amines relaxes with increasing temperature.

To complete these experiments, T_1 ^{13}C NMR relaxation measurements were conducted on the cellulose-*6MDA* complex. The evolution of the sample magnetization, and thus the evolution of its molecular mobility, by choosing the C4 and C6 carbons of cellulose (*i.e.* Figure 1) and the carbons immediately adjacent to the $-NH_2$ functions for *6MDA* was considered. All samples magnetization were normalized (*i.e.* M_0) to that obtained for measurements with a delay acquisition time of 0.00001s. An example of the evolution of the chosen carbons normalized magnetization M/M_0 for the cellulose-*6MDA* complex characterized at 23°C as a function of the delay acquisition time is shown in Figure 6.

Figure 6 shows three mayor relaxation time regimes for the diamine carbons and the C6 of cellulose, and two regimes for the C4 of cellulose. The first regime τ_1 has a very short relaxation time (*i.e.* less than a second) for both the diamine and cellulose and can be attributed to fast local motions withing the carbons. The second τ_2 and third τ_3 regimes have relaxation times varying from the tens of second (diamines and C6 of cellulose) to the hundreds of seconds (cellulose). These relaxation regimes are a signature of molecular motions within the complex (*i.e.* relaxation times of the diamines and cellulose)

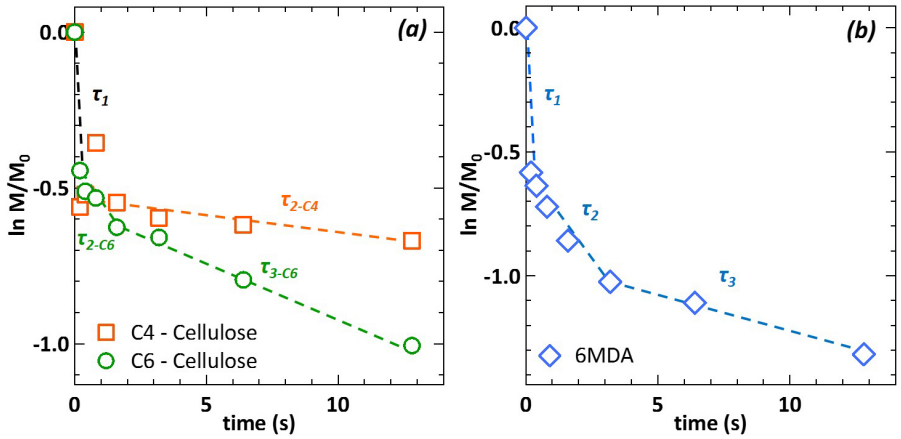

Fig. 6 Normalized magnetization relaxation as a function of the delay obtained by T_1 ^{13}C NMR experiments time for (a) the C4 carbon of cellulose (i.e. Figure 1) and (b) the carbons immediately adjacent to the $-NH_2$ functions for *6MDA*. Dashed lines are exponential fits allowing the extraction of τ_1, τ_2, and τ_3 relaxation times listed in Table 4.

and can be indirectly linked to the mobility observed by *2D WISE* ^{13}C NMR measurements. The numerical values of τ_1, τ_1, and τ_1 were obtained by fitting each regime with an exponential function. These values, obtained at 23, 75, and 90°C, are listed in Table 4.

Table 4 τ_1, τ_2, and τ_3 relaxation regime times obtained for the C4 and C6 of Cellulose (*i.e.* Figure 1) and for the carbons immediately adjacent to the $-NH_2$ functions in *6MDA* in the Cellulose-*6MDA* complex obtained by T_1 ^{13}C NMR experiments at 23, 75 and 90°C.

		T_1 relaxation times (s)		
Relaxation regime	Temperature (°C)	Cellulose Carbons		Diamine Carbon
		C4	C6	Adjacent to $-NH_2$
τ_1	23	0.450	0.667	0.386
	75	0.368	0.560	0.308
	90	0.366	0.540	0.282
τ_2	23	1480	750	5.9
	75	400	7.3	3.2
	90	49	3.7	2.5
τ_3	23	-	-	38.4
	75	-	17.6	8.9
	90	-	6.4	-

From Table 4, it can be observed for the carbons in *6MDA* that their τ_2 and τ_3 relaxation times diminish, and even disappear when the temperature rises. This is a clear indication that the molecular mobility of this diamine increases with temperature. Then, for cellulose, it is seen in Table 4 that the C4 carbon has a relatively long τ_2 relaxation time which remains constant with increas-

ing temperature. This means that this carbon remains rigid in the range of considered temperatures. In the case of the C6 carbon, it is observed that τ_2 and τ_3 relaxation times, albeit larger than those of the diamine, diminish with increasing temperature. This may be due to the fact that H bonds between diamines and cellulose are formed mostly through this carbon. As vicinal diamines relax with increasing temperature, so would this carbon, which is also the most mobile of all cellulose carbons. This could be thus considered as a signature of the beginning of cellulose molecular relaxations activated by the presence of diamines and by an rise in temperature.

3.4 Molecular mobility by MDSC

Finally, the molecular mobility at a macroscopic scale was assessed by Modulated DSC for cellulose-diamine complexes containing either *EDA*, *6MDA*, and *7MDA*. By analyzing the Reversing Heat Flow [52, 53, 54] and the derivative of the Reversing Thermal Capacity C_P with temperature [51] it was possible to dissociate the phenomena responding in phase with the modulated ramp (*i.e.* glass transition temperature T_g) from kinetic phenomena (*i.e.* melting, chemical reactions, solvent evaporation, oxidation, etc.). Glass transitions appear as steps on the Reversing Heat Flow and as peaks on the derivative of the Reversing Thermal Capacity C_P with temperature. Figure 7 shows a thermogram plotting both signals as a function of temperature for the cellulose-*6MDA* complex.

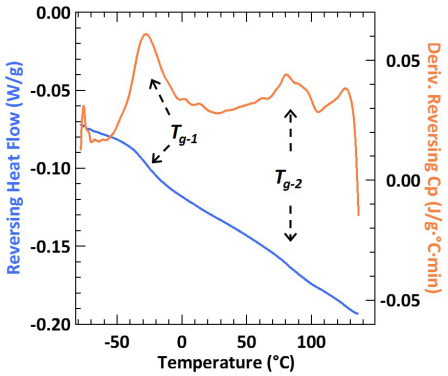

Fig. 7 Reversing Heat Flow and Derivative of the Reversing Thermal Capacity C_P with temperature as a function of temperature obtained by MDSC for the cellulose-6MDA sample highlighting the presence of two transition temperatures T_g. Data is plotted with EXO UP notation.

As shown in Figure 7, two transition temperatures T_g were observed for the three studied complexes, their values are listed in Table 5.

Table 5 shows that T_{g-1} (herein named sub-zero T_g) seems to be independent of the diamine as regards 6MDA and 7MDA and that its temperature

Table 5 Glass transition temperatures T_g measured by Modulated DSC for selected cellulose-diamine complexes.

Cellulose complex	T_{g-1} (°C)	T_{g-2} (°C)
Neat	-	-
+ EDA	0.1 ± 0.4	93.1 ± 4.1
+ 6MDA	-24.5 ± 3.2	83.8 ± 2.8
+ 7MDA	-27.1 ± 5.1	78.1 ± 0.7

range for the three cellulose-diamine complexes is similar to that of the T_g measured for HDPE as mentioned in section 3.3, *i.e.* between -20 and 0°C [63]. T_{g-2} (herein called high temperature T_g) on the other hand seems to depend on the diamine length. Indeed, the larger the diamine in the complex, the lower T_{g-2}.

From these measurements, and in combination with the results observed by by *2D WISE* and T_1 ^{13}C NMR through a multiscale approach, the following origin of these two glass transition temperatures is proposed :

- The sub-zero T_g would correspond to the relaxation motions internal to the diamines chemical structure that are activated at temperatures between -20 and 0°C as in the case of HDPE [63], as diamines in the studied complexes are highly constrained by celullose chains.
- The high temperature T_g would correspond to the motion of cellulose-diamine planes, which can be liked to the fact that at temperatures of 70°C and above, a rise in molecular mobility in diamines and on the *C6* cellulose carbon was observed by ^{13}C NMR measurements. Moreover, this tempertaure is related to the diamine size in each complex. Indeed, the larger the diamine, the easier it would be to induce the motion of cellulose-diamine planes as cellulose chains are further separated from each other, thus requiring less energy (*ergo* temperature) to induce these motions.

To summarize this analysis, Figure 8 shows schematically the molecular origin of both glass transition temperatures.

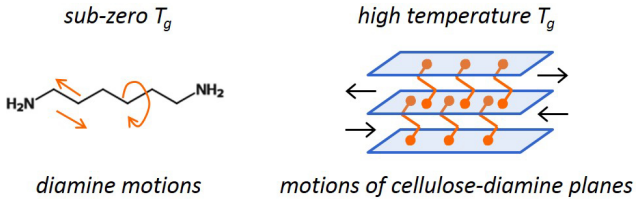

Fig. 8 Proposed origin of the two glass transition temperatures T_g observed by Modulated DSC in combination with molecular mobility phenomena observed by *2D WISE* and T_1 ^{13}C NMR measurements.

4 Conclusion

In this work, the influence of a series of diamines in the structure and the molecular mobility of cellulosic complexes was investigated. It was shown that the presence of such molecules has a notable influence on cellulose structure. For instance, X Ray diffraction experiments demonstrated that the (010) crystallographic plane of the monoclinic unit cell increases almost linearly with the size of diamines, and the unit cell angle γ diminishes and tends towards 90° when the diamine molecular size increases, leading to a crystal structure variation from a monoclinic to an orthorhombic cell. Moreover, solid-state ^{13}C *CP-MAS* NMR showed that complexes with even-numbered diamines induce mostly an "ordered" structure phase in cellulose whereas odd-numbered diamines yield a majoritarian "disordered" structure. Afterwards, *2D WISE* and T_1 relaxation time solid-state ^{13}C NMR experiments revealed that between 23 and 90°C molecular movements can be observed and characterized within the cellulose-diamine. Finally, Modulated DSC evidenced two glass transition temperatures in cellulose-diamine complexes. Through a multiscale approach combining the results from this technique to those obtained by ^{13}C NMR, the sub-zero T_g was attributed to relaxation motions internal to the diamines chemical structure, while the high temperature T_g was attributed correspond to the motion of cellulose-diamine planes.

Conflict of interest

The authors declare that they have no conflict of interest.

References

1. M. Gericke, J. Trygg, P. Fardim, Chemical reviews **113**(7), 4812 (2013). DOI https://doi.org/10.1021/cr300242j
2. M.M. Reddy, S. Vivekanandhan, M. Misra, S.K. Bhatia, A.K. Mohanty, Progress in polymer science **38**(10-11), 1653 (2013). DOI https://doi.org/10.1016/j.progpolymsci.2013.05.006
3. I. Diddens, B. Murphy, M. Krisch, M. Müller, Macromolecules **41**(24), 9755 (2008). DOI https://doi.org/10.1021/ma801796u
4. A. Pinkert, K.N. Marsh, S. Pang, M.P. Staiger, Chemical reviews **109**(12), 6712 (2009). DOI https://doi.org/10.1021/cr9001947
5. K. Mazeau, L. Heux, The Journal of Physical Chemistry B **107**(10), 2394 (2003). DOI https://doi.org/10.1021/jp0219395
6. K. Mazeau, Cellulose **12**, 339 (2005). DOI https://doi.org/10.1007/s10570-005-2200-5
7. M. Calahorra, M. Cortazar, J. Eguiazábal, G. Guzmán, Journal of Applied Polymer Science **37**(12), 3305 (1989). DOI https://doi.org/10.1002/app.1989.070371203

8. J. Schroeter, F. Felix, Cellulose **12**, 159 (2005). DOI https://doi.org/10.1007/s10570-004-0344-3
9. H. Wang, G. Gurau, R.D. Rogers, Chemical Society Reviews **41**(4), 1519 (2012). DOI https://doi.org/10.1039/C2CS15311D
10. J. Wu, J. Bai, Z. Xue, Y. Liao, X. Zhou, X. Xie, Cellulose **22**, 89 (2015). DOI https://doi.org/10.1007/s10570-014-0502-1
11. I.M. Klotz, J.S. Franzen, Journal of the American Chemical Society **84**(18), 3461 (1962). DOI https://doi.org/10.1021/ja00877a009
12. S. Gill, L. Noll, The Journal of Physical Chemistry **76**(21), 3065 (1972). DOI https://doi.org/10.1021/j100665a027
13. R.F. Hopmann, The Journal of Physical Chemistry **78**(23), 2341 (1974). DOI https://doi.org/10.1021/j150671a009
14. W.L. Jorgensen, C.J. Swenson, Journal of the American Chemical Society **107**(6), 1489 (1985). DOI https://doi.org/10.1021/ja00292a007
15. Y. Numata, H. Kono, S. Kawano, T. Erata, M. Takai, Journal of bioscience and bioengineering **96**(5), 461 (2003). DOI https://doi.org/10.1016/S1389-1723(03)70132-7
16. M. Wada, L. Heux, Y. Nishiyama, P. Langan, Cellulose **16**, 943 (2009). DOI https://doi.org/10.1007/s10570-009-9338-5
17. Y. Ishikura, Journal of materials science **46**(11), 3785 (2011). DOI https://doi.org/10.1007/s10853-011-5292-3
18. L. Segal, L. Loeb, Journal of Polymer Science **42**(140), 351 (1960). DOI https://doi.org/10.1002/pol.1960.1204214006
19. X. Su, S. Kimura, M. Wada, S. Kuga, Cellulose **18**, 531 (2011). DOI https://doi.org/10.1007/s10570-011-9505-3
20. M. Wada, G.J. Kwon, Y. Nishiyama, Biomacromolecules **9**(10), 2898 (2008). DOI https://doi.org/10.1021/bm8006709
21. Y. Nishiyama, M. Wada, B.L. Hanson, P. Langan, Cellulose **17**, 735 (2010). DOI https://doi.org/10.1007/s10570-010-9415-9
22. W. Davis, A. Barry, F. Peterson, A. King, Journal of the American Chemical Society **65**(7), 1294 (1943). DOI https://doi.org/10.1021/ja01247a012
23. J.J. Creely, L. Segal, L. Loeb, Journal of Polymer Science **36**(130), 205 (1959). DOI https://doi.org/10.1002/pol.1959.1203613017
24. J. Creely, R. Wade, Textile Research Journal **45**(3), 240 (1975). DOI https://doi.org/10.1177/004051757504500309
25. J. Creely, R. Wade, A. French, Textile research journal **48**(1), 37 (1978). DOI https://doi.org/10.1177/004051757804800106
26. Z. Wang, S. Liu, Y. Matsumoto, S. Kuga, Cellulose **19**, 393 (2012). DOI https://doi.org/10.1007/s10570-012-9651-2
27. L. Segal, Journal of Polymer Science Part A: General Papers **2**(6), 2951 (1964). DOI https://doi.org/10.1002/pol.1964.100020643
28. L. Segal, F. Eggerton, Journal of Polymer Science Part A: General Papers **2**(11), 4845 (1964). DOI https://doi.org/10.1002/pol.1964.100021115
29. S.P. Chundawat, G. Bellesia, N. Uppugundla, L. da Costa Sousa, D. Gao, A.M. Cheh, U.P. Agarwal, C.M. Bianchetti, G.N. Phillips Jr, P. Langan, et al., Journal of the American Chemical Society **133**(29), 11163 (2011).

DOI https://doi.org/10.1021/ja2011115
30. M. Wada, Y. Nishiyama, G. Bellesia, T. Forsyth, S. Gnanakaran, P. Langan, Cellulose **18**, 191 (2011). DOI https://doi.org/10.1007/s10570-010-9488-5
31. H. Chanzy, Cellulose **18**(4), 853 (2011). DOI https://doi.org/10.1007/s10570-011-9547-6
32. R. Parthasarathi, G. Bellesia, S. Chundawat, B. Dale, P. Langan, S. Gnanakaran, The Journal of Physical Chemistry A **115**(49), 14191 (2011). DOI https://doi.org/10.1021/jp203620x
33. Y. Nishiyama, P. Langan, H. Chanzy, Journal of the American Chemical Society **124**(31), 9074 (2002). DOI https://doi.org/10.1021/ja0257319
34. Y. Nishiyama, J. Sugiyama, H. Chanzy, P. Langan, Journal of the American Chemical Society **125**(47), 14300 (2003). DOI https://doi.org/10.1021/ja037055w
35. Y. Nishiyama, G.P. Johnson, A.D. French, V.T. Forsyth, P. Langan, Biomacromolecules **9**(11), 3133 (2008). DOI https://doi.org/10.1021/bm800726v
36. Y. Nishiyama, Journal of wood science **55**(4), 241 (2009). DOI https://doi.org/10.1007/s10086-009-1029-1
37. M. Wada, T. Okano, J. Sugiyama, Journal of Wood Science **47**(2), 124 (2001). DOI https://doi.org/10.1007/BF00780560
38. D.L. VanderHart, R. Atalla, Macromolecules **17**(8), 1465 (1984). DOI https://doi.org/10.1021/ma00138a009
39. T. Mori, E. Chikayama, Y. Tsuboi, N. Ishida, N. Shisa, Y. Noritake, S. Moriya, J. Kikuchi, Carbohydrate polymers **90**(3), 1197 (2012). DOI https://doi.org/10.1016/j.carbpol.2012.06.027
40. H. Kono, S. Yunoki, T. Shikano, M. Fujiwara, T. Erata, M. Takai, Journal of the American Chemical Society **124**(25), 7506 (2002). DOI https://doi.org/10.1021/ja010704o
41. H. Kono, Y. Numata, Polymer **45**(13), 4541 (2004). DOI https://doi.org/10.1016/j.polymer.2004.04.025
42. L. Heux, E. Dinand, M. Vignon, Carbohydrate Polymers **40**(2), 115 (1999). DOI https://doi.org/10.1016/S0144-8617(99)00051-X
43. P. Wormald, K. Wickholm, P.T. Larsson, T. Iversen, Cellulose **3**, 141 (1996). DOI https://doi.org/10.1007/BF02228797
44. P.T. Larsson, K. Wickholm, T. Iversen, Carbohydrate research **302**(1-2), 19 (1997). DOI https://doi.org/10.1016/S0008-6215(97)00130-4
45. P.T. Larsson, E.L. Hult, K. Wickholm, E. Pettersson, T. Iversen, Solid state nuclear magnetic resonance **15**(1), 31 (1999). DOI https://doi.org/10.1016/S0926-2040(99)00044-2
46. K. Wickholm, P.T. Larsson, T. Iversen, Carbohydrate Research **312**(3), 123 (1998). DOI https://doi.org/10.1016/S0008-6215(98)00236-5
47. W.L. Earl, D.L. VanderHart, Journal of the American chemical society **102**(9), 3251 (1980). DOI 10.1021/ja00529a064
48. W.L. Earl, D. VanderHart, Macromolecules **14**(3), 570 (1981). DOI 10.1021/ma50004a023

49. K. Schmidt-Rohr, H.W. Spiess (eds.), *Multidimensional Solid-State NMR and Polymers* (Academic Press, London, 2005)
50. C. Hodgman (ed.), *CRC Handbook of Chemistry and Physics 44th Edition* (CRC Press, Cleveland, 1962)
51. Y. Pang, D. Jia, H. Hu, D. Hourston, M. Song, Journal of applied polymer science **74**(12), 2868 (1999). DOI https://doi.org/10.1002/(SICI)1097-4628(19991213)74:12<2868::AID-APP10>3.0.CO;2-%23
52. A. Rios de Anda, L.A. Fillot, S. Rossi, D. Long, P. Sotta, Polymer Engineering & Science **51**(11), 2129 (2011). DOI https://doi.org/10.1002/pen.22064
53. A. Rios de Anda, L.A. Fillot, F. Preda, S. Rossi, D. Long, P. Sotta, European polymer journal **55**, 199 (2014). DOI https://doi.org/10.1016/j.eurpolymj.2014.04.001
54. A. Rios de Anda, L.A. Fillot, D.R. Long, P. Sotta, Journal of Applied Polymer Science **133**(21) (2016). DOI https://doi.org/10.1002/app.43457
55. M. Koham (ed.), *Nylon Plastics Handbook* (Carl Hanser Verlag, Munich, 1995)
56. J. Puiggalí, L. Franco, C. Alemán, J. Subirana, Macromolecules **31**(24), 8540 (1998). DOI https://doi.org/10.1021/ma971895b
57. M. Mizuno, A. Hirai, H. Matsuzawa, K. Endo, M. Suhara, M. Kenmotsu, C.D. Han, Macromolecules **35**(7), 2595 (2002). DOI https://doi.org/10.1021/ma011839h
58. E. Badea, G. Della Gatta, D. D'Angelo, B. Brunetti, Z. Rečková, The Journal of Chemical Thermodynamics **38**(12), 1546 (2006). DOI https://doi.org/10.1016/j.jct.2006.04.004
59. S. Marčelja, The Journal of Chemical Physics **60**(9), 3599 (1974). DOI https://doi.org/10.1063/1.1681578
60. K. Uno, Y. Ogawa, N. Nakamura, Crystal Growth and Design **8**(2), 592 (2008). DOI https://doi.org/10.1021/cg700729q
61. V.R. Thalladi, R. Boese, H.C. Weiss, Angewandte Chemie (International ed. in English) **39**(5), 918 (2000). DOI https://doi.org/10.1002/(sici)1521-3773(20000303)39:5<918::aid-anie918>3.0.co;2-e
62. J.L. Hallary, F. Lauprêtre, L. Monnerie (eds.), *Polymer Materials, Macroscopic Properties and Molecular Interpetrations* (John Wiley & Sons, Hoboken, 2010)
63. K. Sewda, S. Maiti, Polymer bulletin **70**, 2657 (2013). DOI https://doi.org/10.1007/s00289-013-0941-0